EPJ Web of Conferences **41**, 03006 (2013)
DOI: 10.1051/epjconf/20134103006

Ultrafast Dynamics of the VO_2 Insulator-to-Metal Transition Observed by Nondegenerate Pump-Probe Spectroscopy

N. F. Brady[1], K. Appavoo[2], M. Seo[3], J. Nag[2], R. P. Prasankumar[3], R. F. Haglund[2], and D. J. Hilton[1]

[1]University of Alabama at Birmingham, Birmingham, Alabama
[2]Vanderbilt University, Nashville, Tennessee
[3]Los Alamos National Laboratory, Center for Integrated Nanotechnology, Los Alamos, New Mexico

Abstract. Non-degenerate pump (1.5 eV)-probe (0.4 eV) transmission spectroscopy on vanadium dioxide films grown on glass and three different sapphire substrates shows systematic variations with substrate that correlate with VO_2 grain size and laser fluence. Temperature dependent measurements showed changes in the electronic response that is proportional to the metallic fraction.

1 Introduction

Vanadium dioxide is a canonical model material for the study of insulator-to-metal transitions (IMTs) in strongly correlated systems. The IMT occurs thermally in bulk materials at a critical temperature (T_c) of 340 K, which is accompanied by a structural phase transition from monoclinic to rutile. An open question is the relative importance of electron correlations and the structural transition on the collapse of the band gap and the formation of the metallic phase [1-2]. The understanding of these properties in thin films is complicated by the spatial in-homogeneity of the IMT [3], the dynamics of nucleation and domain growth after photoexcitation or heating [4], and the influence of disorder and defects on the transition [5]. The influence of disorder on the insulator-to-metal phase transition in vanadium dioxide is well established [6], but there has been no comprehensive investigation of the influence of morphology and grain structure on the electronic properties and the optically induced phase transition.

2 Substrate Dependent Pump-Probe Spectroscopy

We have performed nondegenerate pump-probe spectroscopy at 300 K in samples grown on different substrates with a variety of morphologies and grain structures. The samples are pumped at 1.5 eV (above band gap) at fluences ranging from 0.28 mJ/cm^2 to 6.16 mJ/cm^2, and probed with time-delayed 0.4 eV pulses (below band gap) derived from an optical parametric amplifier. Samples were grown by pulsed laser deposition on glass and three different orientations of sapphire (a-, c- and r-cut corresponding to the $(11\bar{2}0)$, (0001), and $(1\bar{1}02)$ planes of the $R\bar{3}c$ space group). VO_2 grown on glass has an initial random orientation, resulting in a disordered crystalline film. The initial growth on sapphire follows the crystalline orientation of the surface plane, resulting in morphological phases exhibiting variable disorder due to the relaxation dynamics from the as-deposited film to the monoclinic VO_2 form upon cooling. Figure 1 (Left) shows scanning electron

microscope images of the surface of each sample/substrate combination and the resulting surface morphologies, highlighting the variations in substrate-dependent structure. Of the crystalline substrates used in this experiment, the lattice mismatch is minimum in case of r-cut sapphire and maximum in case of a-cut sapphire. The a-cut sapphire sample supports longer and broader single crystals of VO_2, while much smaller out-of-plane cylindrical grains are seen for films on r-cut sapphire. Atomic force microscopy on these films shows that both a-cut and c-cut sapphire have a lateral correlation length of ~ 500 nm^2, whereas the correlation length measured on r-cut substrates is a factor of ten smaller. Since the phase transition in a thin film is a composite process of nucleation of the phase transition at the grain boundary or other defects and its propagation throughout each grain, the phase transition dynamics and fluence thresholds should be strongly dependent on the crystalline growth conditions.

Figure 1(right (a)) shows the measured differential transmission at a pump fluence of F=0.28 mJ cm^{-2}. These data all exhibit results consistent with state filling in a semiconductor (subpicosecond lifetimes) and an overall rise in free carrier absorption in each substrate. The minimum in the differential transmission is substrate dependent at this fluence and from lowest to highest it is a-cut (-2.3×10^{-3}), glass (-1.52×10^{-3}), c-cut (-1.51×10^{-3}), and r-cut (-1.2×10^{-3}). The strong substrate dependence using F=1.12 mJ cm^{-2}, shown in Figure 1 (right (b)), suggests that the threshold to nucleate new metallic islands in the parent semiconducting phase varies for each crystalline

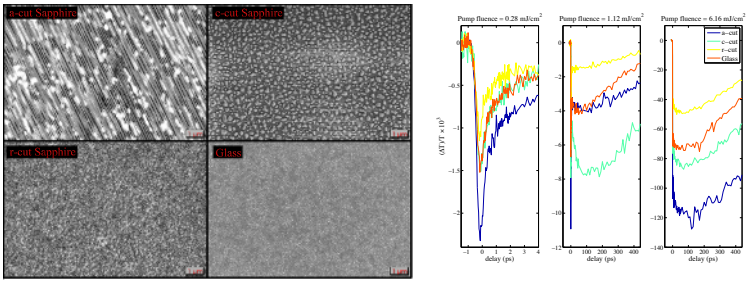

Fig. 1. Left: Electron microscope image of our four VO_2 samples grown at the same time on different substrates. All of the samples are 80 nm thick and grown on a-cut, c-cut, r-cut sapphire and glass, respectively. The films on sapphire are epitaxial and grown at 500°C deposition temperature. Right: Room temperature nondegenerate pump-probe spectroscopy of VO_2 on different substrates with 1.55 eV pump and 0.4 eV probe.

orientation. In the r-cut substrate, these results are again consistent with photogeneration of carriers in a semiconductor, suggesting that the nucleation threshold is higher in this sample than in the glass, a-cut and c-cut samples, where initial subpicosecond dynamics are followed by a secondary decrease in differential transmission that indicates the formation of additional metallic islands within the parent phase. Figure 1 (right (c)) shows the measured data at 6.16 mJ cm^{-2}, which shows an overall larger magnitude and show similar dynamics of metallic nucleation and island growth in the parent phase as the threshold fluence for inducing long range metallic phase is approached. We note the similarity in pump probe dynamics at 1.12 mJ cm^{-2} for the a- and c-cut substrates, which have similar crystalline features, and the comparative difficulty driving the phase transition in the r-cut substrate, which has substantially smaller grains. This suggests that the measured dynamics may be closely related to the intra-grain growth rate of the metallic phase.

3 Temperature Dependent Pump-Probe Spectroscopy

Another experiment focuses on the temperature dependent effect on the nucleation and grown of metallic domains. We pumped the sample with wavelength λ_{pump} = 800 nm (1.55 eV), which gives

sufficient energy to create e-h pairs in the semiconducting phase. Probing with energy below the band gap, λ_{probe} = 3.1 μm (0.4 eV), we obtain metallic properties of the sample. We performed these experiments at the Center for Integrated Nanotechnologies and obtained relaxation dynamics of VO_2, as shown in Figure 2 (left). This data set has three regions of interest; a high temperature bulk metallic phase, a low temperature bulk insulating phase, and a near threshold mixed phase. The mixed phase is of interest due to Qazilbash[3] postulating a novel metal phase existing in this region unlike the bulk high temperature metal phase. We have modeled the low temperature phase, high temperature phase, and mixed phase to $g_1(t)$ (Equation 1), $g_2(t)$ (Equation 2), and $g_3(t)$ (Equation 3) respectively. As shown in Figure 2 (right) the C parameter scales with temperature and is proportional to the metallic fraction.

$$g_1(t) = u(t)\left[(B_1 - B_1 e^{-\frac{t}{\tau_a}}) + (B_2 - B_2 e^{-\frac{t}{\tau_b}}) + (B_3 - B_3 e^{-\frac{t}{\tau_c}})\right] e^{-\frac{t}{\tau_1}} \quad (1)$$

$$g_2(t) = u(t)\left[e^{-\frac{t}{\tau_2}} + A_1 e^{-\frac{t}{\tau_3}}\right]\left[(B_4 - B_4 e^{-\frac{t}{\tau_d}}) + (B_5 - B_5 e^{-\frac{t}{\tau_e}})\right] \quad (2)$$

$$g_3(t) = C_1 g_1(t) + (1 - C_1) g_2(t) \quad (3)$$

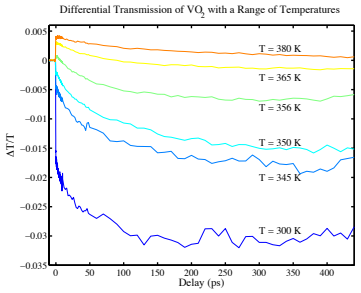

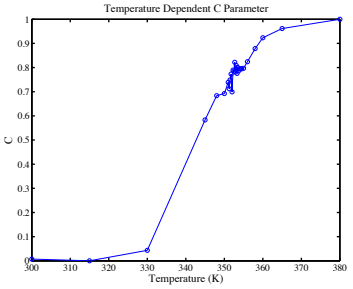

Fig. 2. Left: Nondegenerate pump-probe spectroscopy of VO_2 with 800 nm (1.55 eV) pump and 3 .1 μm (0.4 eV) probe. A subset of the data is shown, highlighting the change from negative differential to positive differential transmission as a temperature increases. Right: C parameter extracted from fitting $g_3(t)$ to the temperature dependent pump-probe spectroscopy on VO_2.

Acknowledgements

This work was performed, in part, at the Center for Integrated Nanotechnologies, a U.S. Department of Energy, Office of Basic Energy Sciences user facility at Los Alamos National Laboratory (Contract DE-AC52-06NA25396) and Sandia National Laboratories (Contract DE-AC04-94AL85000). NFB acknowledges support from the US Dept. Education GAANN Fellowship (P200A090143). KA, JN and RFH acknowledge support from the Office of Science, U. S. Department of Energy (DE-FG02-01ER45916).

References

1. Cavalleri, A. *et al*. Physical Review B **70**, 161102 (2004).
2. Pashkin, *et al*., Physical Review B **83**, 195120 (2011).
3. M. M. Qazilbash, *et al*. Science **318**, 1750 (2007); Qazilbash et al. Physical Review B 77, 115121 (2008).
4. Hilton, D.J. *et al*. Physical Review Letters **99**, 226401 (2007).
5. Appavoo, K. *et al*., Nano Letters **12**, 780 (2012)
6. Goodenough., J. Journal of Solid State Chemistry **3**, 490 (1971).